

## Experimental Investigations Heat Transfer and Pressure Drop Characteristics of Flow Through Circular Tube Fitted With Drilled Cut-Conical Rings

Ameer A. Jadooa\*

Received on: 20/9/2010

Accepted on: 3/2/2011

### Abstract

The heat transfer rate and pressure drop characteristics of turbulent flow of air through uniformly heated circular tube fitted with drilled cut conical rings with three space ratios ( $X=5.4, 6.4, \text{ and } 8.4$ ) have been studied experimentally. The flow characteristics are governed by space ratio (the ratio of the distance between drilled conical ring and the inner diameter of tube), Reynolds number, and drilled conical ring diameter to inner diameter of tube. The goal of the present work is to investigate the effect of drilling of the cut conical ring turbulators (with constant ring to tube diameter ratio) and space ratio on heat transfer, friction factor, and enhancement efficiency under ranging of Reynolds number from 5000 to 23500. In addition, correlation for Nusselt number, friction factor and performance evaluation criteria to assess the real benefits in using the drilled-conical ring turbulator of the enhanced tube are determined. The results show that the process of drilling of the conical ring inside tube gives high rates of heat transfer more than that in the conical ring without drilling.

### دراسة عملية لخصائص انتقال الحرارة وفرق الضغط لجريان الهواء المضطرب خلال انبواب دائري مجهز بحلقات مخروطية مقطوعة مثقبة

#### الخلاصة

تم اجراء دراسة عملية لخصائص انتقال الحرارة و فرق الضغط لجريان الهواء المضطرب خلال انبواب دائري مجهز بحلقات مخروطية مقطوعة مثقبة بثلاث نسب للمسافة (5.4, 6.4, 8.4). الجريان الحاكمة هي نسبة المسافة (النسبة بين المسافة بين الحلقات المخروطية و القطر الداخلي للانبوب). الهدف من الدراسة الحالية التحري عن تأثير ثقب الحلقات المخروطية المقطوعة التي تسبب الاضطراب (نسبة قطر الحلقة الى الانبوب ثابتة) و نسبة المسافة على عملية انتقال الحرارة, معامل الاحتكاك, وكفاءة التحسين تحت مدى  $Re$  يمتد من 5000 الى 23500. اضافة الى ذلك, يتم استنباط معادلات تجريبية لرقم  $Nu$ , معامل الاحتكاك, و معيار الاداء لمعرفة الفوائد الحقيقية من استخدام مضطربات مخروطية مثقبة للانبوب المحسن. بينت النتائج ان عملية ثقب الحلقات المخروطية يعطي معدلات عالية لانتقال الحرارة اكثر من تلك التي تعطيها الحلقات المخروطية غير المثقوبة.

### 1. Introduction

In the past decade, heat transfer enhancement technology has been developed and widely applied to heat exchanger applications; for example,

refrigeration, automotives, process industry, solar water heater, etc. The aim of augmentative heat transfer is to accommodate high heat fluxes. Up to date, there has been a great attempt to reduce the sizes and cost of the

heat exchanger, and energy consumption. The cost of significant variable in reducing the size and the cost of the heat exchanger is a heat transfer coefficient and a pressure drop, which greatly leads to less capital cost and to another advantage of a reduction in the temperature driving force, which increases the second law efficiency and decreases entropy generation. Thus, this captivates the inserts of the number of researchers **Eiamsa-ard et al, 2006**. The passive technique includes the use of treated surfaces, rough surfaces, extended surfaces, displaced enhancement devices, coiled tubes, additives for liquids and gases and swirl flow devices **Rayb and Date, 2003**. Convective heat transfer in a tube with turbulator inserts is dynamically different from the one without turbulator. The heat transfer process with turbulator includes the effects of increased turbulence due to spiraling flow, increased circulation created with heating due to large centrifugal force and turbulator effects. The reverse flow, sometimes called "re-circulation flow", device or the turbulator is widely employed in heat transfer engineering applications. The effect of reverse flow and boundary layer disruption (dissipation) is to enhance the heat transfer coefficient and momentum transfers. The reverse flow with high turbulence flow can improve convection of the tube wall by increasing the effective axial Reynolds number, decreasing the cross section flow area and increasing the mean velocity and temperature gradient. It can help to produce higher heat fluxes and momentum transfers not only due to

the large effective driving potential force but also the higher pressure drop. The strength of the reverse flow and the reattachment position are the main inserts in many heat transfer applications such as heat exchangers, combustion chambers, gas turbine blades and electronic devices.

**Saha et al, 1989** proved experimentally that the heat transfer process in a tube fitted with regularly spaced twisted tape elements connected by thin circular rods is better than full length twisted tapes at high Reynolds number, high twists, and small spacing. **Kumar and Prasad, 2000** improved the heat transfer rates in a solar water heater collectors by inserting twisted tape throughout it, to increase by 18-70%. Experimental studies conducted by **Shou-Shing Hsieh et al, 2003** to enhance heat transfer by a factor 16 of laminar flow in horizontal tube using longitudinal inserts. The heat transfer rates from using both nozzle-turbulators, were found by **Promvonge and Eiamsa-ard, 2006** to be higher than that from the plain tube at a range of 236 to 344%. **Naga Sarada et-al, 2009** observed that the enhancement of heat transfer by using mesh inserts when compared to plain tube at the same mass flow rate in more by a factor of 2 times where as the pressure drop is only about a factor of 1.45 times. **Thianpong et al, 2009**, studied experimentally friction and compound heat transfer behaviors in a dimpled tube fitted with a twisted tape swirl generator, and show that the heat transfer coefficient and friction factor in the combined devices increase as the pitch ratio and twist ratio decrease. **Seemawute and Eiamsa-ard, 2010** conducted an experiment using water

as a testing fluid flows through a uniform heating circular tube fitted with perpherlly-cut twisted tape with alternate axes. They showed that the heat transfer rates in the tube fitted with peripherally-cut alternate-axes twisted tape was enhanced up to 184% of heat in the plain tube.

In some of the above literature review, most the conical-ring turbulators are in truncated hollow cone shape with constant thickness throughout with convergent and divergent arrangements. None of them are drilled conical-ring (nozzle geometry). In the present work, the conical-rings have many holes distributed in uniform distances above the conical ring with the same number for each ring. The strength level of the turbulence flow is generated from the separation and the vortex generated throughout the holes along the tube axes.

**2. Experimental Setup**

A schematic of the experimental setup is shown in Fig.(1). The setup consisted of a blower, orifice meter to measure the air flow rate, and the heat transfer test section. The steel test tube had a length of L=1200mm, with 50mm inner diameter (D), 55mm outer diameter (D<sub>o</sub>) and 5mm tube thickness (t). The tube was heated by continuously wound flexible electrical wire, which provided uniform heat flux boundary condition. The electrical output power was controlled by a variac transformer to obtain a constant heat flux along the entire length of the test section. In order to reduce axial conduction of heat at the ends of the test sections, Teflon discs of thickness 50mm each were used on either side of the test sections. The

inlet and outlet air temperature were measured by multi-channel with chrome-alumel thermocouple (type k). It was necessary to measure the temperature at 15 stations altogether at the outer surface of the tube for finding out the local and average Nusselt number. The entrance and the exit of the tube were provided with pressure tapings for measuring the pressure drop by connecting to the U-tube manometer. In the experiments, the drilled conical-ring turbulators used in the present are depicted in Fig.(2). The drilled conical-ring was made of aluminum with 50 mm (1.0D) in length and its small end diameter (d) was 24mm (0.432D), with a 1.4mm uniform thickness.

**3. Data Reduction**

**Data Reduction**

In the present work, air is used as the tested fluid and flowed through a uniform heat flux and insulated tube. The heat flux of the wall was calculated from the equation

$$Q = \dot{m} C_p (T_{bo} - T_{bi}) \quad \dots(1)$$

The bulk temperature of the fluid at any axial position along the tube axis was computed by assuming a linear temperature variation along the length since the experiment results show that the temperature distribution along the tube is linear. The steady state of the heat transfer rate is established after 2-3 hours. In this state, all thermocouple readings were noted. The heat transfer coefficient by convection from the test section can be written as:

$$h = \frac{Q}{A(T_{ave} - T_b)} \quad \dots(2)$$

where

$$T_{ave} = \frac{\sum_{i=1}^{18} T_{w_i}}{18} \quad \dots(3)$$

and

$$T_b = \frac{T_{bi} + T_{bo}}{2} \quad \dots(4)$$

$T_{w_i}$  Is the local surface temperature at the outer wall of the inner tube. The average surface temperature  $T_{ave}$  is calculated from 18 points of  $T_w$  lined between the inlet and the exit of the test tube.

The average Nusselt number, Nu is estimated as follows:

$$Nu = \frac{h.D}{\kappa} \quad \dots(5)$$

The Reynolds number is given by:

$$Re = \frac{U.D}{\nu} \quad \dots(6)$$

The friction factor ( $C_f$ ) can be written as:

$$C_f = \frac{\Delta P}{(L/D)(\rho U^2 / 2)} \quad \dots(7)$$

Where U is the mean air velocity in the tube. All of the thermophysical properties of the air are determined at the overall bulk temperature from Eq.(4).

The enhancement efficiency ( $\psi$ ) is defined as the ratio of the heat transfer coefficient for the tube fitted with drilled conical-ring ( $h_c$ ) or conical ring alone to that for the plain tube ( $h_p$ ) at a constant Reynolds number (CR) as follows **Yakut et al,2004**:

$$\psi = \frac{h_c}{h_p} |_{CR} \quad \dots(8)$$

#### 4. Results and Discussion

##### 4.1 Validation of plain tube data

Fig.(3) shows the variation of

Nusselt number with Reynolds number for plain tube .the experimental data are matching with the previous correlations under a similar condition (**Incropera and Dewit, 1996** ) with the discrepancy of less than  $\pm 6.5\%$  .

The variation of friction factor with Reynolds number for plain tube is shown in Fig.(4). The present plain tube data is found to be in good agreement with previous correlations of ( $Nu=0.03277Re^{0.742}Pr^{0.4}$  ,  $f=0.6165Re^{-0.317}$ ) from the open literature (**Promovong & Petukov**) within  $\pm 5.8\%$  deviation.

##### 4.2 Effect of Drilled Conical-Ring on Heat Transfer Augmentation

Heat transfer results of the tube fitted with drilled conical ring are shown in Fig.(5) in which the mean Nusselt number are higher than that in the plain tube (empty tube) .It is noticed also that the average Nusselt number increases as the space length between the conical-rings decrease (i.e., as the number of the drilled conical ring increases) and as the Reynolds number increases. From the experimental results, it is clear that the conical ring inserts increase the area of heat transfer from one hand and reverse the flow inside tube from the other hand leads to enhance convection heat transfer. The using of holes on the surface of conical ring will help the flow to pass through it at high velocities to impact at the wall of tube. As a sequence, the tube wall will cold at high rates. On other words, the drilled conical-ring turbulator is employed to create a recirculating near the wall regime leading to redeveloping of thermal boundary layer. These phenomena result in a better mixing of the flow between the wall and the core

regions, and this mixing increase as the number of conical rings increase.

**4.3 Effect of Drilled Conical-Ring on Friction Factor**

Fig.(6) presents the variation of the friction factor with Reynolds number. As can be seen, the friction factor decreases with increase in Reynolds number. The friction factor for drilled conical-ring is higher than the plain tube and the smaller space length between the conical rings leads to higher friction factor because of the dissipation of dynamic pressure of the fluid due to higher surface area and the act caused by the reverse flow.

**4.4 Performance Evaluation Analysis**

The quality of enhancement concept is derived from the performance ratio. Fig.(7) represents the variation of performance ratio (enhancement efficiency) with Reynolds number. The performance ratio obtained with s/D=5.4, 6.4, and 8.4. It shows that the enhancement efficiency increases with reduction of the ratio of s/D, especially at lower Reynolds number. This can expressed that the conical-ring turbulators are not feasible in terms of energy saving at higher Reynolds number values.

**4.5 Correlations For Drilled Conical-Ring**

Based on the present data of the tube fitted with drilled conical ring, Nusselt number, friction factor and enhancement efficiency correlations are derived in the following forms, respectively:

$$Nu=1.725Re^{0.891}(d/D)^{-1.012}(s/D)^{0.011} \dots(9)$$

$$C_f=18Re^{-0.11}(d/D)^{-1.11}(s/D)^{-0.121} \dots(10)$$

$$\psi=9.987Re^{-0.112}(d/D)^{-0.0121} \dots(11)$$

Figs.(8 and 9) show comparisons between the present experimental data and the presents predictions. In the figures, results of the present work reasonably agree well with the available correlations within ±7.8% in comparison with experimental data for the Nusselt number and within ±8.1% for the friction factor.

**5. Conclusions**

1-The experimental investigation has been performed with enhancement devices (drilled conical-ring) for enhancing heat transfer rate in a constant heat flux circular tube.

2-The drilling of conical ring which is fitted with a tube has significant effect on the enhancement of heat transfer because of high flow mixing process.

3-Emperical equations for the Nusselt number, friction factor and enhancement efficiency are deduced to use in the direct applications

4-Despite very high friction, the turbulators (drilled conical-ring) can be applied effectively in places where pumping power is not significantly taken into account but the compact size including case of manufacture installation is required.

**Nomenclature**

- A heat transfer area, m<sup>2</sup>
- C<sub>f</sub> friction factor
- C<sub>p</sub> specific heat of air, J/kg.K
- d small end diameter of conical ring, m
- D inner diameter of test tube, m
- h heat transfer coefficient, W/m<sup>2</sup>.K
- κ thermal conductivity of air, W/m.K
- L length of test tube, m
- l conical ring length, m
- ṁ mass flow rate, kg/s
- Nu Nusselt number

$\Delta P$  pressure drop, Pa  
 Pr Prandtl number  
 Q heat flow rate, W  
 Re Reynolds number  
 t thickness of test tube, m  
 T temperature, °C  
 s space between rings, m  
 U mean axial velocity, m/s  
 X space ratio  
 $\Psi$  Thermal enhancement efficiency  
 $\nu$  kinematics viscosity, m<sup>2</sup>/s  
 $\rho$  density, kg/m<sup>3</sup>  
 $\mu$  dynamic viscosity, Ns/m<sup>2</sup>

Subscripts

a air  
 ave average  
 b bulk  
 CR constant Reynolds number  
 i inlet  
 m mean  
 o outlet  
 p plain tube

References

**Date, A. W.**, "Prediction of fully developed flow in a tube containing a twist-tape", *Int. J. Heat Mass Transfer*, Vol.17, 1974, pp. 845-859.

**Eiamsa-ard, S., Thianpong, C., and Promvonge, P.**, "Experimental investigation of heat transfer and flow friction in a circular tube fitted with regularly spaced twisted tape elements", *International Communications in Heat and Mass Transfer*, Vol. 37, Issue 10, December 2006, pp. 1225-1233.

**Kumar, A., and Prasad, B. N.**, "Investigation of twisted tape inserted solar water heaters-heat transfer, friction factor and thermal performance results", *Renewable Energy*, Vol. 19, Issue 3, March 2000, pp. 379-398.

**Incropera F., and Dewit P. D.**, "Introduction to heat transfer", 3<sup>rd</sup> edition, John Wiley & Sons Inc, 1996.

**Promvonge, P. , and Eiamsa-ard, S.**, "Heat transfer and turbulent flow friction in a circular tube with conical-nozzle turbulators", *International Communications in Heat and Mass Transfer*, Vol. 33, Issue 6, 2006, pp. 591-600.

**Naga Sarada, S., Kalyani K. Radha and Raju, A. V. S.**, "Experimental investigations in a circular tube to enhance turbulent heat transfer using mesh inserts", *ARPN journal of Engineering and Applied Sciences*, Issn 1819-6608, Vol. 4, No. 5, July 2009, pp.53-60.

**Rayb S. and Date A.W.**, "Friction and heat transfer characteristics of flow through square duct with twisted tape insert.", *Int. J. Heat Mass Transfer* 2003;46(5):889-902.

**Saha, S. K., Gaitonde, U. N., and Date, A. W.**, "Heat transfer and pressure drop characteristics of laminar flow in a circular tube fitted with regularly spaced twisted tape elements", *Experimental Thermal and Fluid Science*, Vol. 2, Issue 3, July 1989, pp. 310-322.

**Seemawute, P. and Eiamsa-ard, S.**, "Thermohydraulics of turbulent flow through a round tube by a peripherally-cut twisted tape with an alternate axis", *International Communications in Heat and Mass Transfer*, Vol. 37, Issue 6, July 2010, pp. 652-659.

**Shou-Shing Hsieh, Ming-Ho Liu, Huang-Hsiu Tsai**, "Turbulent heat transfer and flow characteristics in a horizontal circular tube with strip-type inserts", Part I, *Fluid Mechanics*, *Int. J. Heat Mass Transfer*, Vol. 46, pp. 823-835, 2003.

**Thiapong, C., Eiamsa, P., Wonggcharee, K., and Eiamsa-ard, S.**, "Compound heat transfer enhancement of a dimpled tube with

a twisted tape swirl generator", International Communications in Heat and Mass Transfer, Vol. 3, Issue 7, August 2009, pp. 698-704.

**Yakut, K., Sahin, B., and Canbazoglu, S.,** "Performance and flow induced vibration characteristics for conical ring turbulators", Applied Energy, 2004; 79(1):65-76.

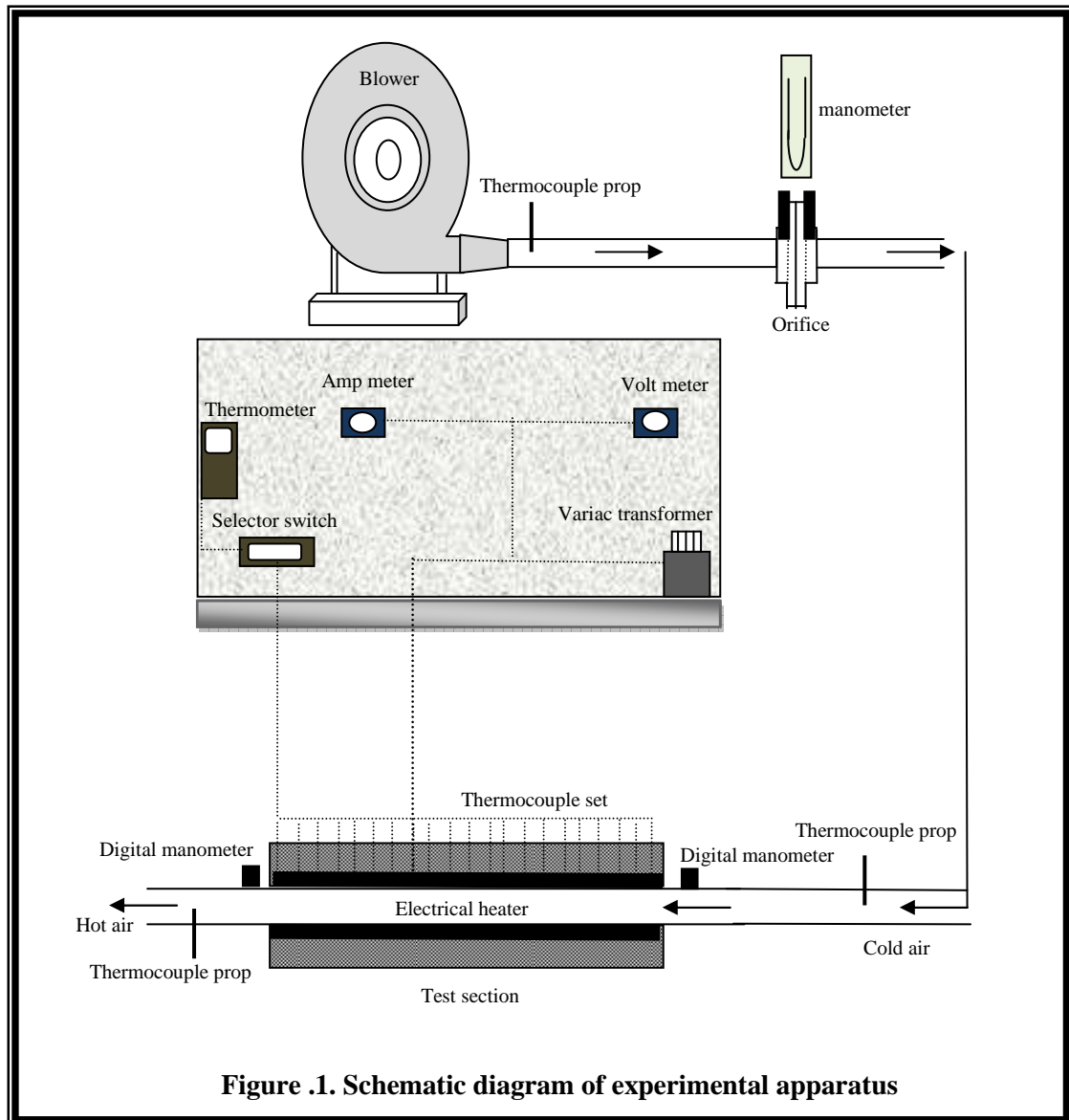


Figure .1. Schematic diagram of experimental apparatus

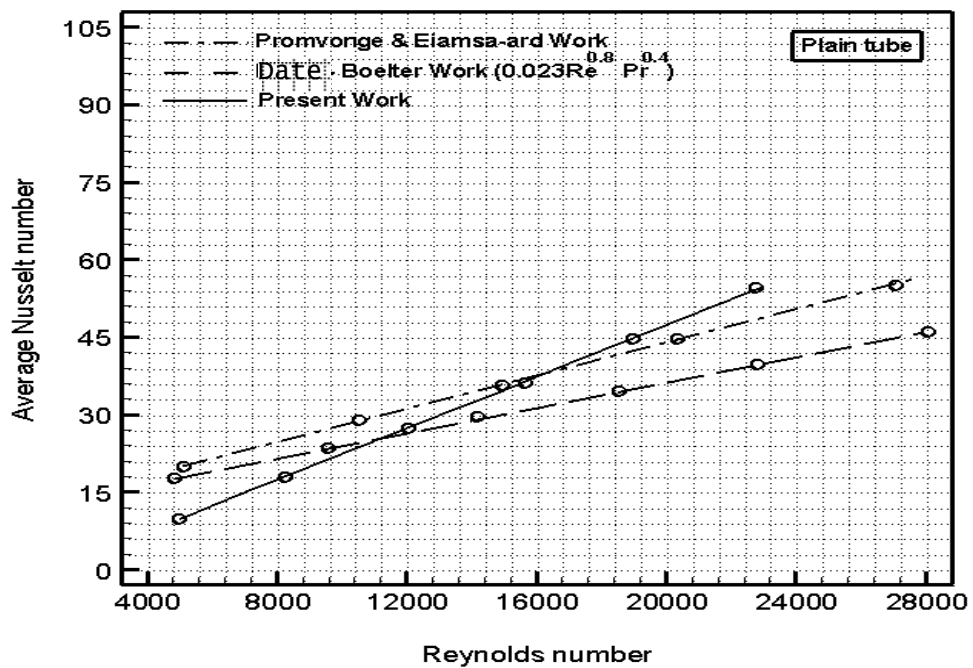
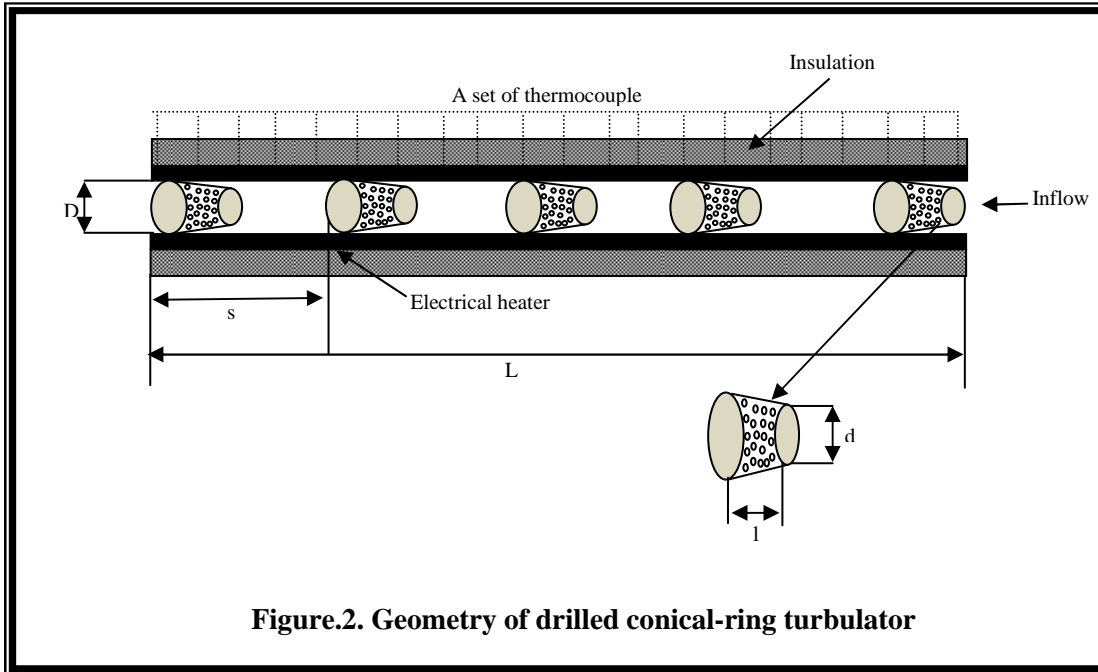


Figure (3): Verification of Nusselt number of plain tube.



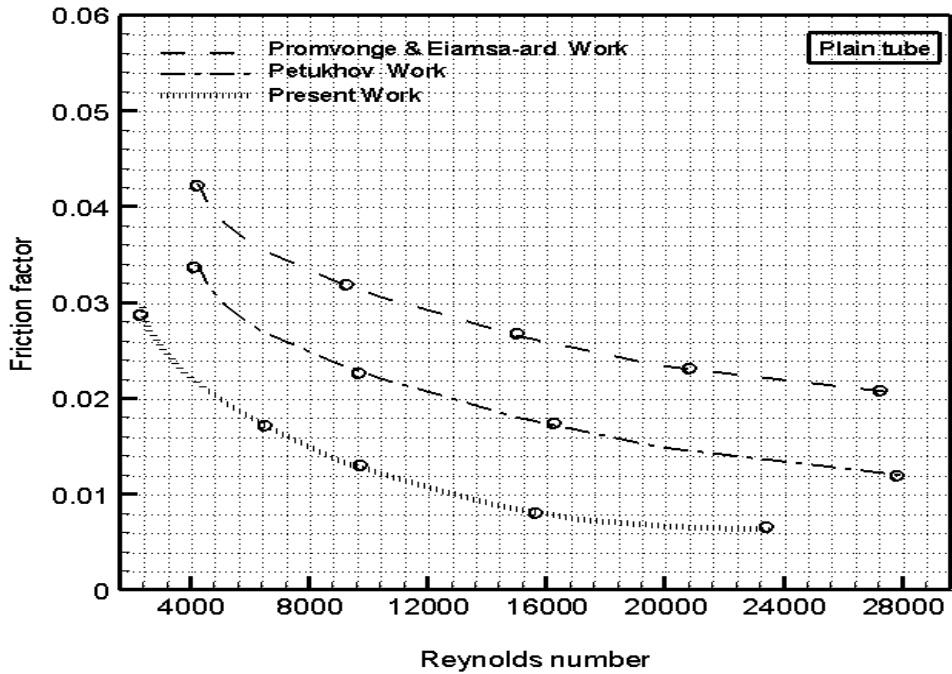


Figure (4): Verification of friction factor of plain tube.

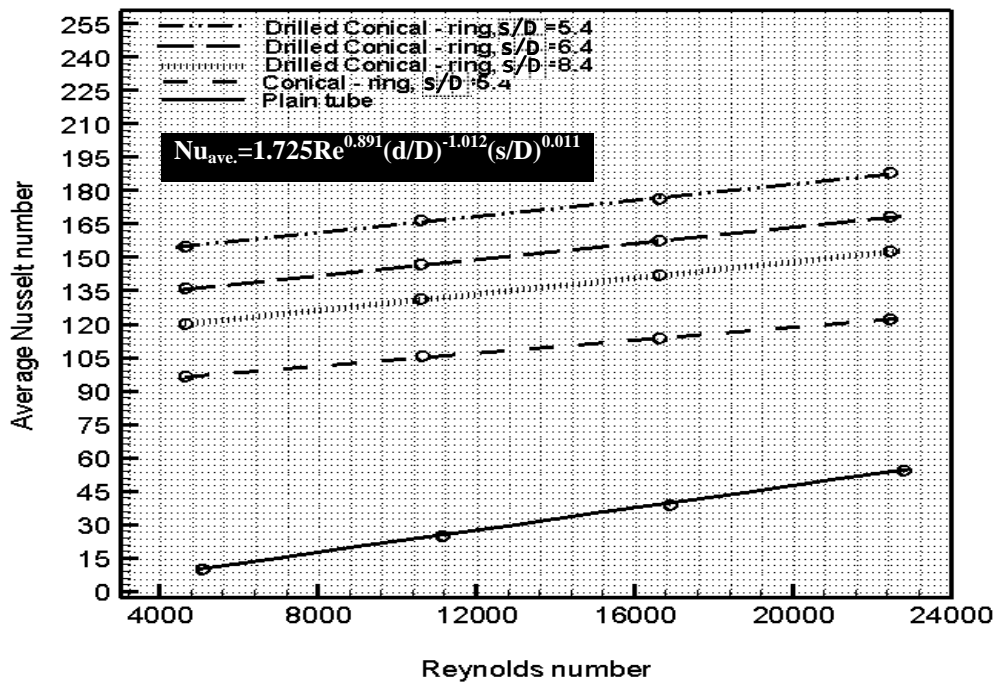


Figure (5): Nusselt number versus Reynolds number with various Drilled conical-ring ratios.

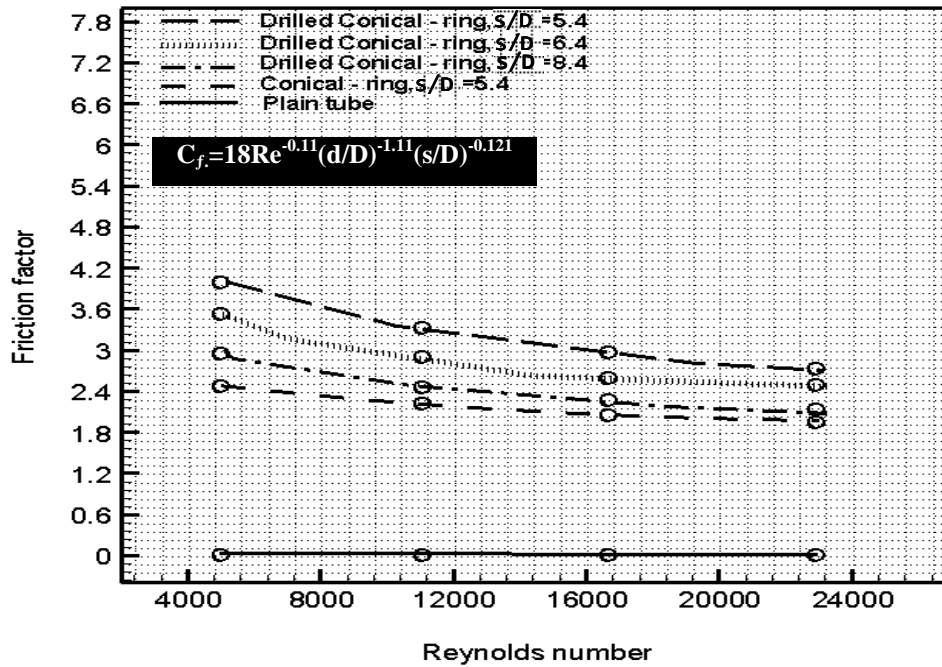


Figure (6): Friction factor versus Reynolds number with various Drilled conical-ring ratios.

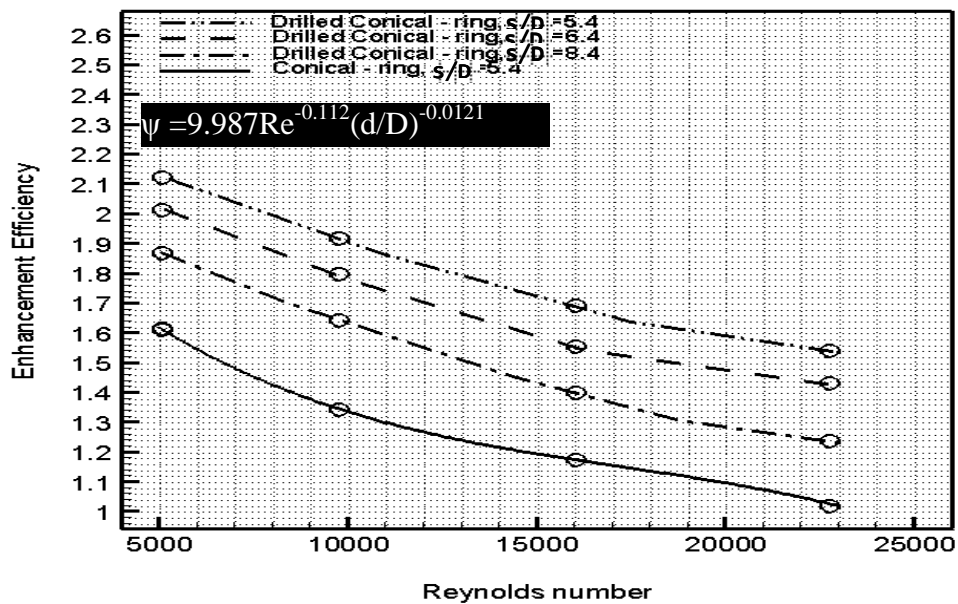


Figure (7): Enhancement efficiency versus Reynolds number with Drilled conical-ring ratios.

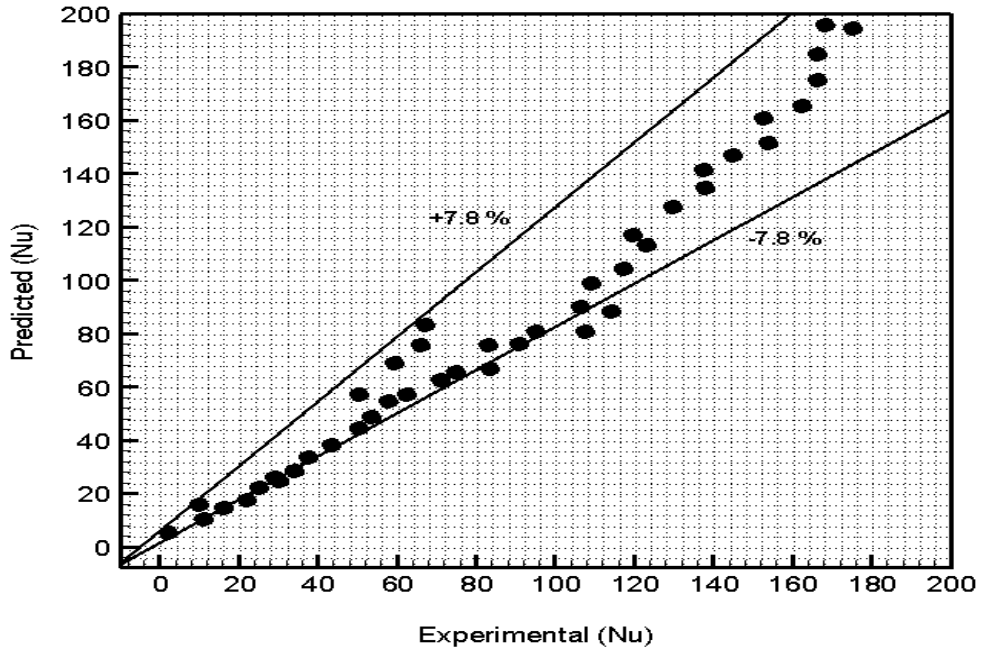


Figure (8): Predicted Nusselt number against experimental Nusselt number.

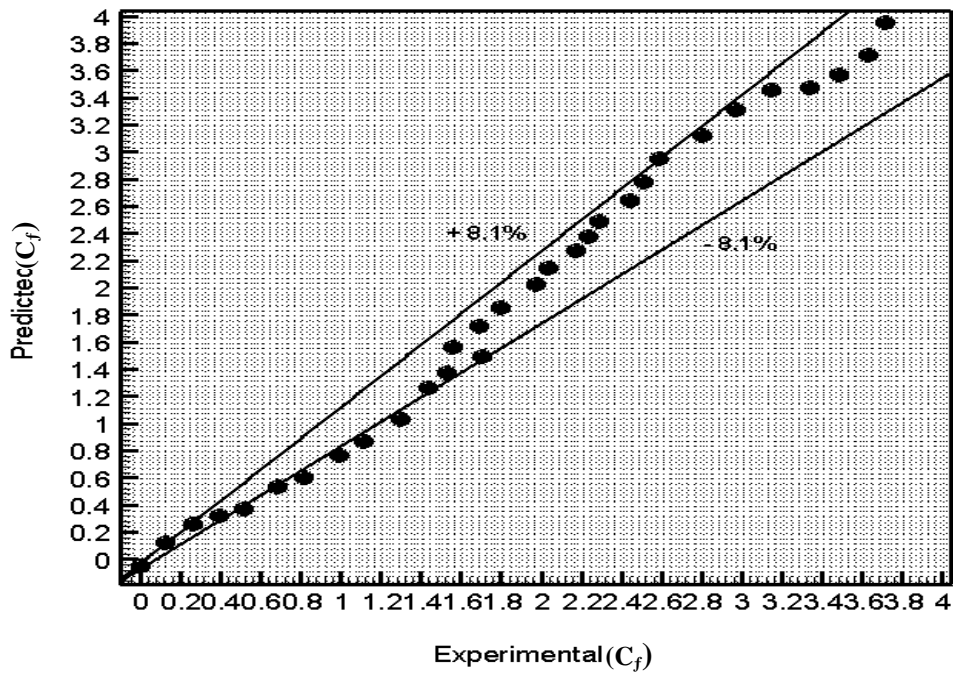


Figure (9): Predicted Friction factor against experimental Friction factor.